

## Magnetization and level statistics at the quantum Hall liquid-insulator transition in the lattice model

M. Niță,<sup>1</sup> A. Aldea,<sup>2\*</sup> and J. Zittartz<sup>2</sup>

<sup>1</sup>National Institute of Materials Physics, P.O. Box MG7, Bucharest-Magurele, Romania

<sup>2</sup>Institut für Theoretische Physik, Universität zu Köln, D-50937 Köln, Germany

(Received 23 September 1999; revised manuscript received 17 April 2000)

Statistics of level spacing and magnetization are studied for the phase diagram of the integer quantum Hall effect in a two-dimensional finite lattice model with Anderson disorder.

The way in which the increasing disorder induces the insulating state when starting from the integer quantum Hall (IQH) state is a topic of controversy between the continuum and lattice models of the two-dimensional (2D) electronic gas in strong magnetic field. The continuum approach predicts the crossover between the adjacent quantum Hall plateaus, ending up with the insulating state when the degree of disorder increases or, equivalently, the limit of small magnetic field is considered. This is due to the so-called “floating up” of the critical energies  $E_c$  which occurs with increasing disorder. ( $E_c$  is the energy where the localization-delocalization transition takes place in the thermodynamic limit.) In the critical region, i.e., when the Fermi energy  $E_f$  crosses an extended state energy  $E_c$ , the transverse (Hall) conductivity is  $\sigma_{xy}^c = \nu - 1/2$  (at the transition between the plateaus  $\nu$  and  $\nu - 1$ ).<sup>1</sup> This means that at large disorder (or low field), the cascade of transitions must end with  $\nu = 1 \rightarrow \nu = 0$  (insulator). The experiments give controversial information in what concerns the possibility to observe this last transition (see Ref. 2 and the references therein, Ref. 3). The sensible conclusion can be found in Refs. 2 and 4 suggesting that the theoretical results of the scaling theory, which are obtained for zero temperature and infinite systems, cannot be checked easily by experiments that are done for finite samples and at low (but nevertheless finite) temperature. The evaluation of the critical value of the longitudinal conductivity is also a difficult task. Lee *et al.*, show in the frame of *corresponding states law* that  $\sigma_{xx}^c = 1/2$  for any  $\nu$ ; approaching the question in the opposite way, Zirnbauer assumes  $\sigma_{xx}^c = 1/2$  and finds agreement with the numerical simulations. The numerical calculation performed by Huo *et al.*, for the lowest Landau level also produces 0.5.<sup>5</sup>

More recently, the same problem has also been approached in lattice models. The results are again controversial, since Yang and Bhatt calculating the Chern numbers for different degrees of disorder, find a tiny floating up of the extended states,<sup>6</sup> while Xie *et al.*, by the study of the localization length, conclude that the positions of extended states remain unchanged as disorder increases. The last authors propose a phase diagram in the energy-disorder plane that allows the direct transition  $\nu \rightarrow 0$ .<sup>7</sup> Unlike Refs. 6 and 7, which use periodic boundary conditions, in this paper we study confined systems by the use of vanishing conditions, so that the Hall current is carried along edge states. The phase diagram obtained here reminds us of one from Ref. 7, however metallic regions (where  $\sigma \neq 0$ ) are implanted in between QH and insulating phases give rise to a crossover.

In this context we study some new relevant features of the disordered lattice model in magnetic field with vanishing boundary conditions, the attention being paid especially to magnetization, level spacing distribution, and conductance on extended states in the so-called metallic region; a comparison with the results obtained by Yang and Bhatt will be done.

The discussion is based on the spinless one-electron Hamiltonian in perpendicular magnetic field defined on a 2D square lattice with  $N$  sites in one direction and  $M$  sites along the other one, which reads as follows:

$$H = \sum_{n=1}^N \sum_{m=1}^M [\epsilon_{nm} |n, m\rangle \langle n, m| + i^{2\pi\phi m} |n, m\rangle \langle n+1, m| + |n, m\rangle \langle n, m+1| + \text{H.c.}], \quad (1)$$

where  $|n, m\rangle$  is a set of orthonormal states, localized at the sites  $(n, m)$ , and  $\phi$  is the magnetic flux through the unit cell measured in quantum flux units. In Eq. (1) the hopping integral at  $\phi = 0$  is taken with unity serving as the energy unit and the diagonal energy  $\epsilon_{nm}$  is a random variable distributed according to the probability density:

$$P(\epsilon) = \begin{cases} 1/W, & -W/2 < \epsilon < W/2 \\ 0, & \text{otherwise.} \end{cases} \quad (2)$$

The averaged spectrum of the Hamiltonian (1) is depicted in Fig. 1 for  $\phi = 1/10$  and the disorder amplitude in the range  $W \in [0, 10]$ . The lines represent the mean eigenvalues  $\langle E_n \rangle$  as a function of disorder amplitude  $W$ .

In order to study the phase diagram we calculate the longitudinal and Hall conductances of this system at constant magnetic flux and varying disorder. The different phases: quantum Hall, metallic, and insulating are characterized not only by conductance but also by the specific distribution of the level spacing and by the current density on the plaquette, described by the operator:

$$J_{nm}^{n'm'} = i t_{nm}^{n'm'} (r_{nm} - r_{n'm'}) |nm\rangle \langle n'm'| + \text{H.c.} \quad (3)$$

(here  $t_{nm}^{n'm'}$  is the hopping integral between the sites  $r_{nm}$  and  $r_{n'm'}$ ).

It is an opportune time to remind previously that for a *clean* system ( $\epsilon_{nm} = 0$ ) with cyclic boundary conditions (i.e., for a torus) and commensurate values of the magnetic flux through the unit cell, the spectrum consists of degenerate bands separated by gaps (the well-known Hofstadter butter-

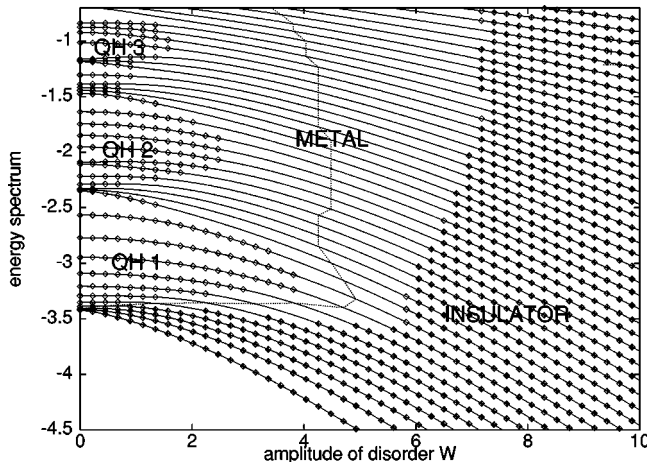


FIG. 1. Phase diagram in the energy-disorder plane. The insulating regime is depicted for  $\sigma_{xx} < 0.2$  and the metallic regime for  $\sigma_{xx} > 0.2$  (in units  $e^2/h$ ). In the QH regime  $\sigma_{xy} = \text{integer}$  and  $\sigma_{xx}$  is negligible. The dotted line in the metallic region corresponds to the critical points where  $\sigma_{xx} = \sigma_{xy}$ . ( $M = N = 10, \phi = 1/10$ .)

fly). However, when vanishing boundary conditions are imposed (i.e., for plaquette<sup>8</sup> or cylinder<sup>9</sup> geometry) the gaps get filled with “edge states”, localized close to the edges of the sample. The other states, the “bulk” ones, remain grouped in bands on the energy scale, while they geometrically are concentrated in the middle of the plaquette. The two types of states differ also by their chirality, i.e., by the sign of the derivative  $dE_n/d\phi$ . The effect on the orbital magnetization of each state is immediate: the expectation values of the operator  $M = \int [r \times j(r)] dS$  calculated on the eigenstates of the Hamiltonian (1) have different signs depending on whether the state is bulk or edge type. Figure 2 shows that the magnetization of the edge eigenstate No. 11 is positive  $M_{11} > 0$ , but the bulk eigenstate No. 12 has  $M_{12} < 0$ ; the local currents corresponding to the two states are also shown in insets. In the same figure one anticipates that the increasing disorder produces a monotonic decrease of the magnetization.

The orbital magnetization of all states in the spectrum is shown in Figs. 3(a) and 3(b) for the clean and disordered system, respectively (the electron-hole symmetry of the Hofstadter spectrum is evident also in the aspect of the magnetization). The disorder effect consisting of the broadening of

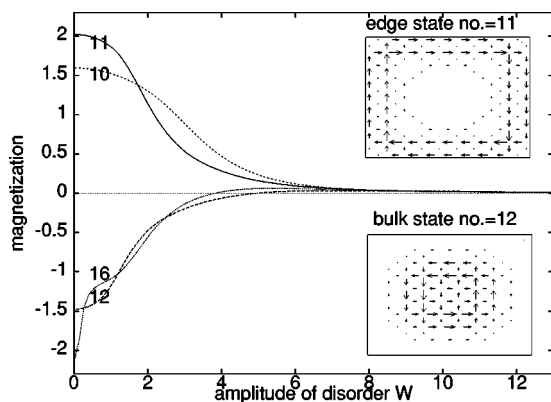


FIG. 2. The decay of the magnetization with increasing disorder for the edge state Nos. 10 and 11 and for the bulk state Nos. 12 and 16. The density of current at  $W=0$  is shown in insets  $\phi = 1/10$ .

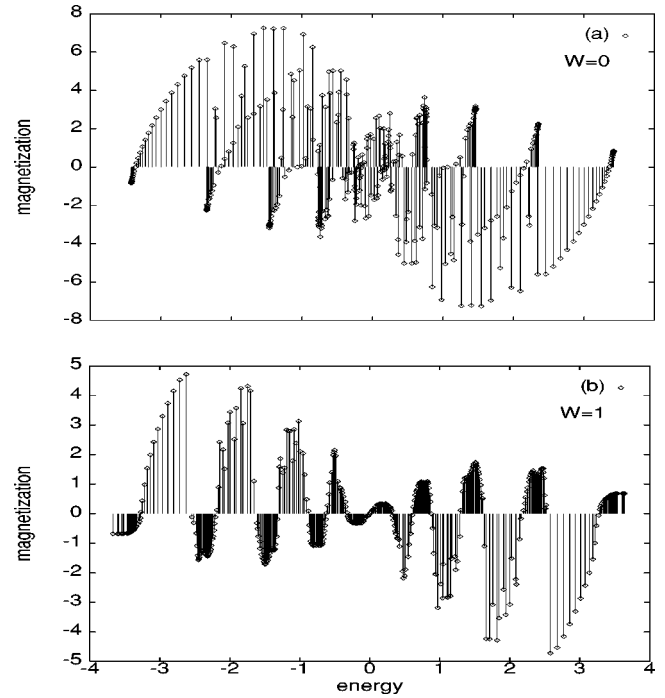


FIG. 3. Magnetization (in arbitrary units) vs energy at  $W=0$  in (a) and  $W=1$  in (b). ( $N=M=20$  and  $\phi = 1/10$ .)

the bands and narrowing of the gaps, is obvious in the second figure. More notable is the magnetization of the ground state  $M_g$ , which can be compared successfully with experimental results. Assuming that the spectrum is filled up to the Fermi energy  $E_f$ , due to the alternating sign of  $M_n$  in different regions of the spectrum, the quantity

$$M_g = \sum_{(E_n < E_f)} M_n, \quad (4)$$

as a function of the number of occupied states, shows a sawtooth aspect (see Fig. 4) which is the same as in the experiments by Wiegiers *et al.*,<sup>10</sup> including the fact that the jumps of  $M_g$  occur at the center of the gaps. In our model, the number of teeth depends on the number of gaps that can be resolved. These de Haas-van Alphen oscillations disappear

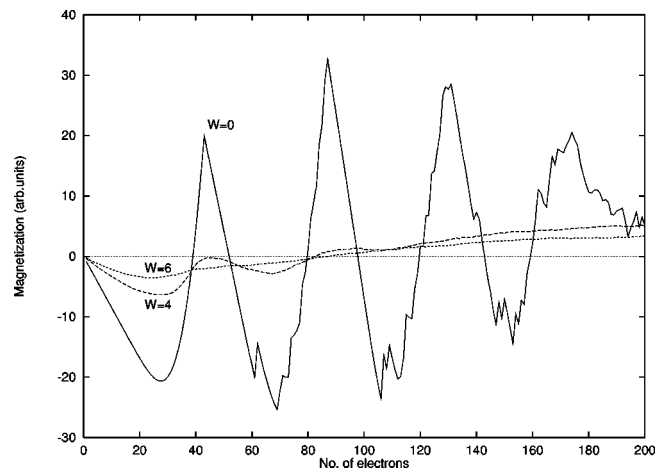


FIG. 4. The ground-state magnetization  $M_g$  vs the number of electrons at different degrees of disorder. ( $N=M=20$ ,  $\phi = 1/10$ .)

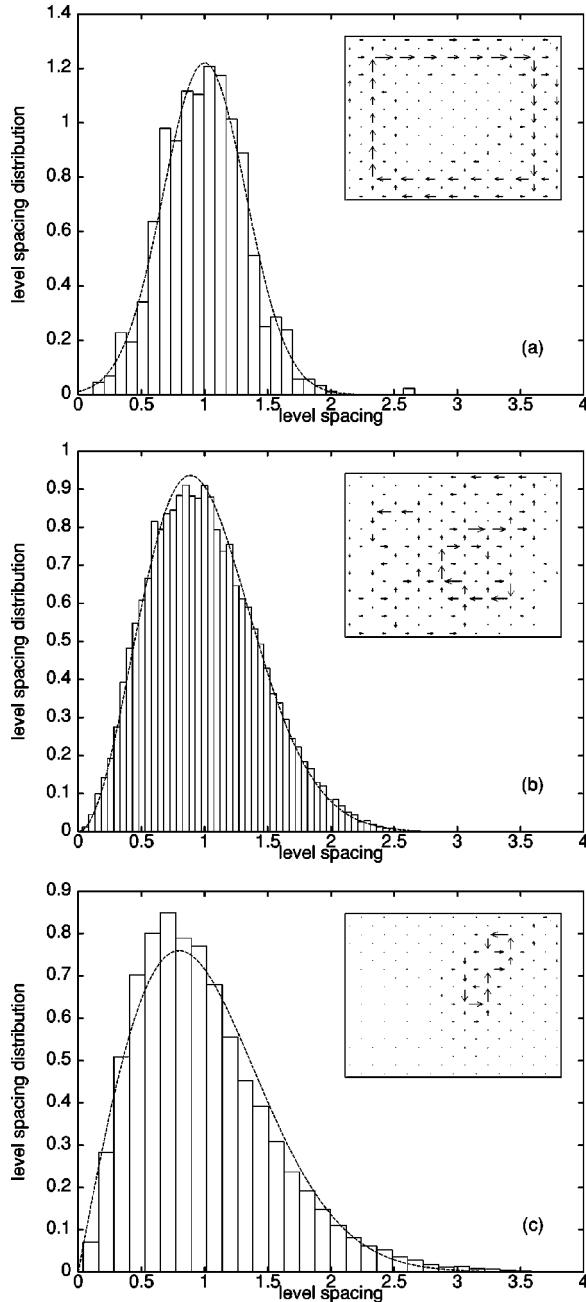


FIG. 5. Level spacing distribution  $\mathcal{P}(t)$  for three typical situations. In (a)  $E \in [-2.9, -2.7]$  and  $W=1$ ; the dotted line is the Gaussian function whose variance equals the calculated variance of the histogram  $\delta(t)=0.33$ . (b)  $\mathcal{P}(t)$  for  $E \in [-2.4, -1.3]$  and  $W=3$ ; the dotted line the Wigner-Dyson distribution with  $\beta=2$ . (c)  $E \in [-2.9, -1]$  and  $W=6$ ; the dotted line is the Wigner-Dyson distribution with  $\beta=1$ . The corresponding typical current densities are shown in insets. ( $N=M=10, \phi=1/10$ , number of configurations = 1000.)

in the metallic regime (see the curves for  $W=4$  and  $W=6$ ); this result can be corroborated with the recent data by Kravchenko *et al.* who found experimentally that the cyclotron minima of the Shubnikov–de Haas oscillations also disappear gradually near the metal-insulator transition in a 2D electron system in silicon.<sup>11</sup>

When the Anderson potential [Eq. (2)] is switched on and  $W$  is increased continuously, the bands become broader and

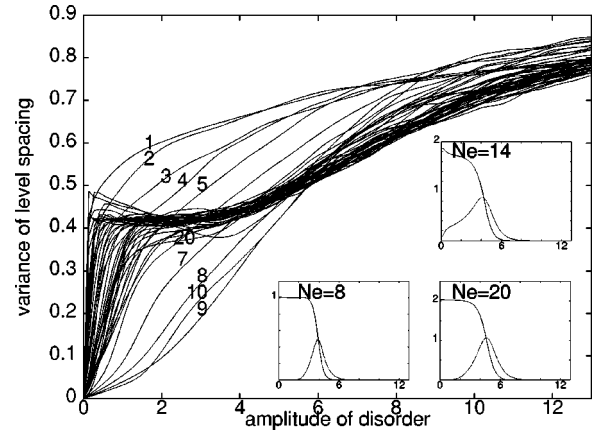


FIG. 6. The variance of level spacing  $\delta(t_n)$  ( $n=1, \dots, 50$ ) vs amplitude of disorder  $W$ . ( $N=M=10$ .) The insets show the evolution of  $\sigma_{xx}$  and  $\sigma_{xy}$  at a given number of electrons  $N_e$  vs  $W$  (for the same plaquette coupled to semi-infinite leads).

broader, the disorder spreads the states over the whole plaquette, giving rise to extended disordered states, and finally produces a quasicontinuum of localized states; even the edge states disappear gradually into the quasicontinuum. The nature of the states can be checked by calculating the distribution  $\mathcal{P}$  of level spacings for various degrees of disorder, in different domains of the spectrum. Let  $s_n$  be the level spacing between two consecutive eigenvalues  $E_n$  and  $E_{n+1}$  and define  $t_n = s_n / \langle s_n \rangle$ , where  $\langle s_n \rangle$  is the mean level spacing.

For infinite systems the level distribution at the transition is a meaningful problem that was first approached (for 3D and zero-magnetic field) by Shklovskii *et al.*<sup>12</sup> For finite systems the crossover of the level statistics between weak and strong localization was discussed by Zharekeshev *et al.*<sup>13</sup> Here we discuss the crossover from IQH to the localized regime for finite 2D systems. The distribution of the spacing between edge levels in the QH regime was not discussed up until now and it is only known that they are more robust against disorder. Our numerical calculation indicates that the distribution function of the distance between two consecutive edge levels is a symmetric curve that can be fitted by a Gaussian [see Fig. 5(a)]. In the insulating phase, the level spacing is described by the Poisson distribution and the crossover between these extreme cases is illustrated in Fig. 6, which shows the variance  $\delta t_n$  for all level spacings of the Hamiltonian (1). One may learn that: (a) at  $W < 4$ , for most of the states,  $\delta t_n \approx 0.42$ , which is the typical value for the unitary Wigner-Dyson (WD) surmise. Indeed, the calculated distribution [Fig. 5(b)] is of this type, proving the presence of extended states in the system with broken time-reversal symmetry. (b) For larger  $W$ , the variance increases towards  $\delta t_n = 1.0$  specific to the Poisson distribution. However, this value cannot be reached practically because of finite dimension of the plaquette. (c) In-between, at  $W \approx 6$ , the variance equals 0.52, which is the typical value for the orthogonal WD distribution. This is an indication that with increasing disorder, the domain of small  $t$ , where the unitary distribution behaves like  $t^2$ , shrinks very much so that  $\mathcal{P}(t)$  may resemble the orthogonal one. The numerical calculated distribution of level spacing can indeed be well-fitted by the orthogonal WD function [see Fig. 5(c) where the linear behavior at small  $t$  is obvious]. (d) The lowest states, originat-

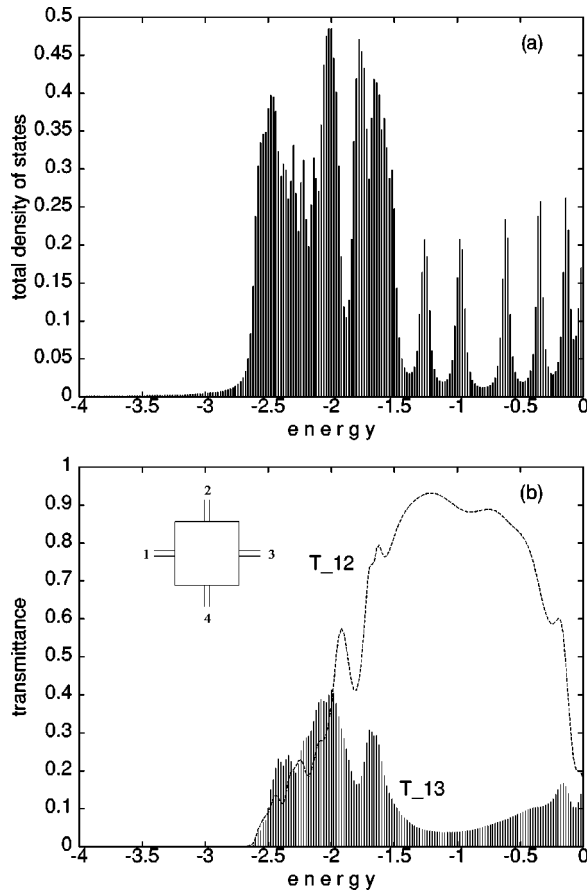


FIG. 7. The total density-of-states for a finite plaquette (a). The transmittances  $T_{12}$  and  $T_{13}$  as function of energy for a plaquette with attached leads (b). ( $N=M=7$  and  $\phi=3/7$ .)

ing from the first band ( $n=1, \dots, 6$ ) get localized faster than the others, while the states from the first gap ( $n=7, \dots, 10$ ) are very robust against the localization process.

At last we discuss some transport properties with special attention to the metallic regime; for this purpose the Landauer-Büttiker formalism and the techniques from Ref. 8 are used after attaching four leads to the plaquette. The con-

ductance in the three different regimes (IQH, metal, and insulator) can be correlated with the spectrum characteristics of the isolated finite system discussed above.

In order to evaluate the role of the boundary conditions, we make a comparison with the paper by Yang and Bhatt, using the same dimensions of the lattice and the same magnetic flux. As in Ref. 6 we calculate the total density-of-states  $\rho$ , however instead of the conducting density-of-states  $\rho_c$ , we calculate separately the transmittances  $T_{12}$  and  $T_{13}$ . Even in the presence of disorder, the bent transmittance  $T_{12}$  is mainly due to the conductance along the edge and is responsible for the Hall effect, while the straight transmittance  $T_{13}$  is due to the delocalized states in the bulk. A correspondence can be established between the three peaks of  $T_{13}$  in Fig. 7 and the three subbands, which under periodic boundary conditions have the Chern numbers  $(-2, 5, -2)$ .<sup>6</sup> The other peaks in  $\rho$  represent edge levels located in the gap where  $T_{12}$  is a maximum but  $T_{13}$  is a minimum. The evolution with disorder of the peaks of  $T_{13}$  is the same as described in Ref. 6 for the conducting density-of-states  $\rho_c$ . On the other hand, the transmittance  $T_{12}$  has a steady position in the gap but gets smaller with increasing disorder. The *monotonic* decrease of  $T_{12}$ , from any given integer  $\nu$  to zero is the cause for the direct transition  $\nu \rightarrow 0$ , which is found for the Hall conductance in numerical calculations based on lattice models for confined 2D electron systems in strong magnetic field.<sup>14</sup>

In conclusion, the metallic regime is characterized by a Wigner-Dyson distribution of the level spacing with  $\beta=2$  (unitary ensemble). As the system evolves versus insulator the distribution resembles the orthogonal WD surmise, indicating the “loss of influence” of the magnetic field. Simultaneously, the orbital magnetization decays to zero. The QH phase is characterized by a Gaussian distribution of spacing between edge levels.

Due to the different chirality of the edge and bulk states, the magnetization of the ground state shows a tooth saw behavior as function of the filling factor, which is attenuated by disorder.

This work was partially performed under SFB 341 of DFG. M.N. thanks the Romanian Academy for their support under Grant No. 69/1999.

\*Permanent address: National Institute of Materials Physics, P. O. Box MG7, Bucharest-Magurele, Romania.

<sup>1</sup>D.E. Khmel'nitskii, Phys. Lett. A **106**, 182 (1984); B. Laughlin, Phys. Rev. Lett. **52**, 2304 (1984); S. Kivelson, D.H. Lee, and S.C. Zhang, Phys. Rev. B **46**, 2223 (1992).

<sup>2</sup>S. Das Sarma, in *Perspectives in Quantum Hall Effects*, edited by S. Das Sarma and Aron Pinczuk (Wiley, New York, 1997).

<sup>3</sup>M. Hilke, D. Shahar, S.H. Song, D.C. Tsui, and H. Xie, preprint cond-mat/9906212 (unpublished).

<sup>4</sup>B. Huckestein, Phys. Rev. Lett. **84**, 3141 (2000).

<sup>5</sup>D.H. Lee, S. Kivelson, and S.C. Zhang, Phys. Rev. Lett. **68**, 2386 (1992); M.R. Zirnbauer, preprint cond-mat/9905054 (unpublished); Y. Huo, R.E. Hetzel, and R.N. Bhatt, Phys. Rev. Lett. **70**, 481 (1993); B. Huckestein and M. Backhaus, *ibid.* **82**, 5100 (1999).

<sup>6</sup>K. Yang and R.N. Bhatt, Phys. Rev. Lett. **76**, 1316 (1996); Phys. Rev. B **59**, 8144 (1999).

<sup>7</sup>D.Z. Liu, X.C. Xie, and Q. Niu, Phys. Rev. Lett. **76**, 975 (1996);

X.C. Xie, D.Z. Liu, B. Sundaram, and Q. Niu, Phys. Rev. B **54**, 4966 (1996).

<sup>8</sup>A. Aldea, P. Gartner, A. Manolescu, and M. Niță, Phys. Rev. B **55**, R13 389 (1997); F. Gagel and K. Maschke, *ibid.* **52**, 2013 (1995).

<sup>9</sup>C. Schulze, J. Hajdu, B. Huckestein, and M. Janssen, Z. Phys. B **103**, 441 (1997).

<sup>10</sup>S.A.J. Wieggers, M. Specht, L.P. Levy, M.Y. Simmons, D.A. Ritchie, A. Cavanna, B. Etienne, G. Martinez, and P. Wyder, Phys. Rev. Lett. **79**, 3238 (1997).

<sup>11</sup>S.V. Kravchenko, A.A. Shashkin, D.A. Bloore, and T.M. Klapwijk, preprint cond-mat/0007003 (unpublished).

<sup>12</sup>B.I. Shklovskii, B. Shapiro, B.R. Sears, P. Lambrianides, and H.B. Shore, Phys. Rev. B **47**, 11 487 (1993).

<sup>13</sup>I.Kh. Zharekesev, M. Batsch, and B. Kramer, Europhys. Lett. **34**, 587 (1996).

<sup>14</sup>D.N. Sheng and Z.Y. Weng, Phys. Rev. Lett. **80**, 580 (1998).